The absence of PNPase activity in Enterococcus faecalis results in alterations of the bacterial cell-wall but induces high proteolytic and adhesion activities

Rabia Ladjouzi, Matthieu Duban, Anca Lucau-Danila, Djamel Drider

The absence of PNPase activity in *Enterococcus faecalis* results in alterations of the bacterial cell-wall but induces high proteolytic and adhesion activities.

Rabia Ladjouzi*, Matthieu Duban, Anca Lucau-Danila, Djamel Drider

UMR Transfrontalière BioEcoAgro N° 1158, Univ. Lille, INRAE, Univ. Liège, UPJV, YNCREA, Univ. Artois, Univ. Littoral Côte d'Opale, ICV – Institut Charles Viollette, F-59000 Lille, France

*** Corresponding author:**

Rabia LADJOUZI. Université de Lille, cité scientifique/Avenue Paul Langevin, Polytech-Lille, Bureau C310. 59655 Villeneuve d'Ascq, France. Email. rabia.ladjouzi@univ-lille.fr

Abstract

Enterococci are lactic acid bacteria (LAB) used as starters and probiotics, delineating their positive attributes. Nevertheless, enterococci can be culprit for thousands of infectious diseases, including urinary tract infections, bacteremia and endocarditis. Here, we aim to determine the impact of polynucleotide phosphorylase (PNPase) in the biology of *Enterococcus faecalis* 14; a human isolate from meconium. Thus, a mutant strain deficient in PNPase synthesis, named *ΔpnpA* mutant, was genetically obtained. After that, a transcriptomic study revealed a set of 244 genes differentially expressed in the *ΔpnpA* mutant compared with the wild-type strain, when exploiting RNAs extracted from these strains after 3 and 6 hours of growth. Differentially expressed genes include those involved in cell wall synthesis, adhesion, biofilm formation, bacterial competence and conjugation, stress response, transport, DNA repair and many other functions related to the primary and secondary metabolism of the bacteria. Moreover, the *ΔpnpA* mutant showed an altered cell envelope ultrastructure compared with the WT strain, and is also distinguished by a strong adhesion capacity on eukaryotic cell as well as a high proteolytic activity. This study, which combines genetics, physiology and transcriptomics enabled us to show further biological functions that could be directly or indirectly controlled by the PNPase in *E. faecalis* 14.

Keywords: polynucleotide phosphorylase (PNPase), transcriptomic analysis, cell envelope alterations, proteolytic activity, cell adhesion

1. Introduction

Polynucleotide phosphorylase (PNPase) is conserved in the course of evolution and therefore is found in different lineages of life as in Bacteria, Archaea, Eukarya, organelles, animals and plants (Leszczyniecka et al., 2004). In terms of its enzymatic activity, two types of reactions associated with PNPase were demonstrated. The first consists in the processive phosphorolytic degradation of mRNA from the 3'-end. Thus, PNPase catalyzes stepwise phosphorolysis of the 3'-terminal phosphodiesters of RNA chains leading to nucleoside diphosphate products (Arraiano et al., 2010). The second consists on a polymerase activity catalyzing reaction using NDPs as substrates to add NMPs to the 3'-end of the RNA chain (Mohanty and Kushner, 2000). The activity of PNPase can be hampered by well-folded RNAs, referred to as double-helical structured RNAs (Spickler and Mackie, 2000). To get over this hurdle, PNPase has a potential to bind to other proteins, forming thereof complex machineries capable of coming through these well-structured RNAs (Arraiano et al., 2010).

In Gram-positive bacteria such as *B. subtilis*, it was established that the formation of the degradosome complex is initiated by RNase Y that binds to exoribonucleases PNPase, to RNase J1 and J2, and then to the other proteins of the complex (Cascante-Estepa et al., 2016; Lehnik-Habrink et al., 2012; Salvo et al., 2016). In *B. subtilis*, the efficient exonucleolytic mRNA decay was found to be dependent on the conjunction of PNPase and helicase CshA (Cardenas et al., 2011), advocating the complexity of the machineries of mRNA degradation. Of note in *Staphylococcus aureus*, PNPase was also shown to interact with RNase Y to degrade transcripts (Numata et al., 2014), whilst in *Streptococcus pyogenes*, PNPase was found to be the main 3′-to-

5′ *in-vivo* exoRNase degrading fragments generated by the RNase Y endoRNases during mRNA decay (Broglia et al., 2020; Lécrivain et al., 2018).

Bacterial species lacking PNPase synthesis are affected in an arc of functions and become unable to execute correctly their genetic programs. In addition to proceed with the possessing of mRNAs in Gram-positive and Gram-negative bacteria, PNPase was shown to be directly or indirectly involved in bacterial responses to cold shock (Zangrossi et al., 2000), cell-competence (Luttinger et al., 1996), biofilm formation (Carzaniga et al., 2012), oxidative and other environmental stress (Wu et al., 2009; Wurtmann and Wolin, 2009), and virulence (Rosenzweig and Chopra, 2013; Sinha et al., 2021). Interestingly, a potential link could exist between PNPase and DNA metabolism as formerly reported, suggesting that PNPase can reversibly catalyze phosphorolysis of ssDNA, and having a role in the DNA repair, mutagenesis and recombination (Becket et al., 2012; Cardenas et al., 2011, 2009; Rath et al., 2012).

In enterococci, only few studies have been conducted on enzymes involved in RNA metabolism. Recently, the role of RNases (J1, J2, III and Y) and three DEAD-box helicases (CshA, B and C) on physiology and virulence of *E. faecalis* was reported (Gao et al., 2017; Salze et al., 2020). In the present work, we focus on the PNPase from *E. faecalis* 14; a strain formerly isolated from meconium (Al Atya et al., 2015). In a first step, we performed a transcriptomic study to identify the genes or network of genes that could be under the direct or indirect control of PNPase, which is known to be a pleiotropic enzyme. For this purpose, we constructed a mutant deficient in PNPase synthesis (*ΔpnpA*) by using the double homologous recombination method. RNAs extracted from the *ΔpnpA* mutant and the WT strains, after 3 and 6 hours of growth were therefore used for this transcriptomic study.

This study clearly shows that the absence of PNPase affects the ultrastructure of the bacterium by altering its cell-envelope, as well as by reducing the size of the cells and colonies. However, these alterations were not detrimental as we recorded better scores of adhesions on Caco-2 eukaryotic cells as well as higher proteolytic activity in the Δ*pnpA* mutant strain than the WT strain. An attempt to link these structural changes and enhanced biological activities through the interpretation of transcriptomic data has been proposed.

2. Materials and methods

2.1. Bacterial strains and growth conditions

Tables 1 and 2 list all bacterial strains, plasmids and primers used in this study. *E. faecalis* 14 cultures were grown at 37 °C in GM17 (M17 medium containing 0.5% (w/v) of glucose). When needed, chloramphenicol (Cm) or erythromycin (Er) antibiotics were added to the media at final concentration of 15 µg ml^{-1} or 150 µg/mL respectively. The agar plates were used for determining the cfu counts. The kinetic growth was performed using the spectrophotometer (Aquoalabo, France) set at an optical density of 600 nm (OD_{600}). *E. coli* strains were grown at 37 °C in Luria-Bertani (LB) broth under aerobic condition with shaking at 160 rpm or on LB agar. When appropriate, ampicillin (100 µg/mL), erythromycin (150 µg/mL) or chloramphenicol (10 µg/mL) was added.

2.2. General molecular methods

Molecular cloning and standard techniques and were routinely performed as described by(Sambrook and Russell, 2001). All enzymes were used in accordance with the manufacturer's instructions and obtained from ThermoFisher Scientific (Courtaboeuf, France). NucleoSpin® kits (Macherey-Nagel, Düren, Germany) was used to purify PCR products and plasmids. All genetic

constructions and the resulting mutants were sequenced (Eurofins, Ebersberg, Germany). SnapGenes tool (GSL Biotech LLC, CA) was used to analyze DNA sequences. Transformation of *E. coli* and *E. faecalis* strains were performed respectively by heat shock and by electroporation using the Gene Pulser Apparatus (Bio-Rad, Hercules, CA, USA).

2.3. Construction of the Δ*pnpA* mutant strain

The Δ*pnpA* mutant strain was constructed by double cross-over using a strategy based on the conditional replication of the pLT06 plasmid (Thurlow et al., 2009), as previously described (Ladjouzi et al., 2020a). Briefly, regions of 953 bp located upstream and 966 bp downstream of the *pnpA* gene were amplified by PCR using the primer pairs *pnp*A-1F /*pnp*A-2R and *pnp*A-3F/*pnpA*-4R respectively (Table 2). The *pnpA*-3F and *pnpA*-2R primers are complementary. The DNA fragment harboring a deletion of 1,148 pb in the N-terminal region of *pnpA* gene was generated with a second PCR using the primers *pnpA*-1F / *pnpA*-4R and the mix of the two previous amplified fragments as DNA template. The resulting DNA fragment of 1.919 bp was cloned into pGEM-t Easy vector (Promega, Madison, WI, USA). The white colonies of *E. coli* XL-1 Blue obtained on LB-X-Gal (40 µg/mL - IPTG (40 µg/mL) containing the recombinant plasmid pGEM-t EasyΔ*pnpA* were selected. The fragment containing mutated *pnpA* gene was extracted from pGEM-t EasyΔ*pnpA* using *Pst*I and *Nco*I restriction enzymes and cloned into the pLT06 plasmid to generate pLT06Δ*pnpA* using the *E. coli* JM109 competent cells for the transformation. The pLT06Δ*pnpA* plasmid was used to transform *E. faecalis* 14 WT and the crossing-over events were induced as previously described (Ladjouzi et al., 2020a). The deletion of the *pnpA* gene was screened by PCR using pnpA5F/pnpA6R or pnpA7F/pnpA8R and confirmed by sequencing.

2.4. Complementation of *E. faecalis* Δ*pnpA* mutant strain

A DNA fragment of 2.32 kb containing the entire *pnpA* gene including the promoter region was amplified by PCR using *pnpA*-CompF and *pnpA*-CompR primers and cloned into pMSP3535 (Tables 1 and 2). The recombinant plasmid pMSP3535:*pnpA* was used to transform *E. faecalis 14* Δ*pnpA* mutant after transformation in *E. coli* XL-1 blue and selection of the positive colonies on LB, Er (150 µg ml^{-1}). After 48 h at 37°C, colonies carrying the recombinant plasmid pMSP3535:*pnpA* were selected on GM17 Er (150 µg/mL) then screened by PCR and sequenced.

2.5. Transmission electron microscopy

For TEM analysis, pellets of WT and its Δ*pnpA* mutant were obtained by centrifugation (8,000 × g, 10 min, 4 °C) of cultures grown on GM17 at 37 °C for 6 h. Pellets were fixed and TEM images were obtained using the same method previously described (Ladjouzi et al., 2020b). An acceleration voltage of 200 KV of the microscope JEOL JEM 2100FX TEM instrument (Jeol, Tokyo, Japan) was used.

2.6. Microarrays analysis and RNA isolation

The microarray analysis was performed using three distinct cultures of *E. faecalis* 14 Δ*pnpA* which were compared with *E. faecalis* 14, after 3 h and 6 h of growth in GM17 medium. Cells were harvested by centrifugation (10,000 × g during 10 min at 4°C) and total RNA was extracted using the NucleoSpinTM RNA Plus columns (Macherey-Nagel, Hoerdt, France). The quantity and quality of RNA samples were determined by capillary electrophoresis, using an

Agilent 2100 Bioanalyzer (Agilent Technologies, France) and a minimal RNA integrity number (RIN) of 8 was required for all samples.

A custom *E. faecalis* 14 oligo-based DNA microarray (8 × 15 K) Agilent G2509F was used to study the gene expression according to the method previously developed in our previous work (Ladjouzi et al., 2020b). Differentially expressed genes (DEGs) were selected when FC threshold > 2.0 or < 0.5 and presented in log2 FC. For the functional annotation of DEGs and relevant biological pathways of selected genes NCBI GenBank, UniProt, AmiGO 2 Gene Ontology and KEGG pathway analysis were used. The microarray data from this study have been submitted to the NCBI GEO with the accession number GSE180397.

2.7. Adhesion to Human Intestinal Cells Caco-2

For the adhesion assay, the human colorectal adenocarcinoma Caco-2 cells were used (Pinto et al., 1983) according to the previously described protocol (Bendali et al., 2011). Briefly, cells were grown at 37 °C and 5% CO2 in Dulbecco's modified Eagle's medium (DMEM) Gibco® (Thermo Fisher Scientific), supplemented with 4.5 g/L glucose, 2 mM L-glutamine, 1% (v/v) non-essential amino acids, 100 U/mL streptomycin, 100 U/mL penicillin, and 10% (v/v) heat-inactivated fetal bovine serum. The reagents used were from PAN-Biotech GmbH (Aidenbach, Germany). To measure the adhesion ability of the bacteria, a culture of 7 days of Caco-2 cells was performed in 24-well tissue culture plates using an inoculum of 5.10^4 cells per well. For the bacteria, 10 mL of overnight cultures of the *E. faecalis* WT and Δ*pnpA* mutant strains grown on GM17 (~ 6.10^9 cfu/mL) were harvested by centrifugation (6,000 x g, 4 °C, 10 min), washed twice with PBS, resuspended in 10 mL of non-supplemented DMEM, and applied to confluent Caco-2 cell monolayers (~ 5.10^5 per well). Volumes of 200 µL and 300 µL

containing 6.10^9 cfu/mL were used. After 2 h of incubation at 37 °C, Caco-2 cell monolayers were washed twice with 500 µL of 10 mM PBS (pH 7.2) to remove non-adherent bacteria. Then, 200 µL trypsin/EDTA Gibco® (Thermo Fisher Scientific) were used to lyse cells for 15 min at room temperature. Finally, the lysates were diluted and the number of adherent bacteria was determined on GM17 agar. Three independent experiments were performed and three replicates by condition were done for each experiment. The percentage of adhesion was determined by the ratio of adherent bacteria/total number of bacteria (control) multiplied by 100.

2.8. CCK-8 cytotoxicity assay

The Cell Counting Kit-8 (CCK-8) assay (Dojindo Molecular Technology, Japan) was used to assess the cytotoxicity of WT and its Δ*pnpA* mutant strains against Caco-2 cells, as previously described (Ladjouzi et al., 2020b). A culture of 7 days of Caco-2 cells at a density of 6×10^4 cells/well was carried out in 96-well cell culture plates using the same conditions as cited above. Overnight cultures grown in GM17 were centrifuged and resuspended in DMEM without antibiotic using the same initial volume. Then, bacteria were added to Caco-2 cell monolayers at a ratio of MOI (Multiplicity of infection) 1:10 (Caco-2/WT or Caco-2/Δ*pnpA* mutant). The non-infected Caco-2 cells were used as control. After 24 h of incubation, cells were washed twice with PBS and incubated for 2 h at 37 °C in 150 µL of DMEM and 5% of CCK-8 reagent. The relative viability (%) of Caco-2 cells was determined by absorbance values at 450 nm using a microplate reader (Xenius SAFAS, Monaco, France). Cytotoxicity levels were expressed as percentage of the viability of the treated Caco-2 cells compared with that of the untreated cells (control).

193
194 **2.9. Proteolytic activity**

195 Cells were harvested by centrifugation (8,000 x *g*/10 min, 4°C) after 18 h of growth at
196 37°C. Then, cells were washed three times with PBS (10 mM, pH 7.2) and resuspended in PBS
197 buffer. A volume of 10 µL of each bacterial strain was plated on nutrient agar (Sigma-Aldrich)
198 supplemented with 10% (w/v) skim milk powder (Sigma-Aldrich) sterilized by autoclaving (110
199 °C/ 10 min, 1 atm), and incubated at 37 °C for 72 h. The appearance of a clear zone around the
200 colonies indicates a proteolytic activity (de Albuquerque et al., 2018).

201
202 **2.10. Statistics**

203 All the results presented in this work were obtained from three independent experiments,
204 and the data are expressed as the mean standard deviation. A *P* value of less than 0.05 is
205 considered to be significant using the Student's test.

206

207 **3. Results**

208 **3.1.Absence of PNPase activity alters the bacterial cell envelope structure and reduces**
209 **the cell size**

210 Growth kinetics performed on GM17 medium at 37 °C for 24 hours revealed that *ΔpnpA*
211 mutant strain has a lower growth performance than the WT strain. After 8 hours of growth, the
212 OD_{600}nm of the WT strain was 3.47 while that of the *ΔpnpA* mutant strain was 2.49, i.e. a ratio of
213 1.54 in favor of the WT strain. The measured growth rates were significantly different (*P*=0.001),
214 based on the statistical values and interpretations. As shown in Fig. 1, the complementation of the
215 *ΔpnpA* mutant strain with *pMSP3535:pnpA,* permitted to recover the phenotype of the WT strain

as well as its growth performances. Statistically, no difference was observed in terms of growth performances, even on other growth media such as BHI, MRS (P=0.001). In addition to the comparison of OD_{600} nm between the WT strain and the *ΔpnpA* mutant, we established a colony count (cfu) after 3, 6, 9 and 24 h of growth and therefore concluded to no significant difference (P> 0.05). The mean count values (cfu/mL) after 3, 6, 9 and 24 h were $3.17x10^8$, $1.26x10^9$, $2.03x10^9$ and $1.40x10^9$ for the Δ*pnpA* mutant and $2.82x10^8$, $1.40x10^9$, $2.15x10^9$ and $1.57x10^9$ for the WT strain respectively. After 24 h of growth, Δ*pnpA* isogenic mutant strain exhibited clearly smaller colonies than the WT (Fig. 2).

Furthermore, TEM analysis performed on both strains after 6 h of growth on GM17 medium (Fig. 3) underpinned as expected typical Enterococci diplococci shape, known as rugby ball forms, but not for the Δ*pnpA* mutant, which displayed severe alterations on the cell envelope. When several cells were viewed together, we noted that most of Δ*pnpA* mutant cells were altered in their cell envelopes and displayed a smaller cell size compared with the WT strain (Fig. 3), arguing on a direct or indirect role of PNPase in this biological pathway.

3.2. Mutant deficient in PNPase synthesis has higher ability of adhesion to eukaryotic Caco-2 cells than the wild-type strain.

TEM analysis enabled to locate alterations in the cell-envelope of the mutant Δ*pnpA*, but not in the WT strain. To see whether such alterations could have any role on the adhesion ability to eukaryotic intestinal Caco-2 cells, adhesion assays were conducted with both strains, using two distinct volumes of 200 µL and 300 µL but a same cell concentration of ~ 6.10^9 cfu/mL. The mutant Δ*pnpA* was significantly more adherent to eukaryotic Caco2 compared with the WT strain. The scores of adhesion registered for the mutant strain were 0.22%±0.015 (200 µL), and

239 0.27% ±0.028 (300 µL), whereas those reported for the WT strain were 0.06%±0.010 (200 µL)
240 and 0.7%±0.010 (300 µL) (Fig. 4). Thus, the mutant Δ*pnpA* was 3.88 (P<0.05) and 3.64 (P<0.05)
241 folds more adherent than the WT with 200 µL or 300 µL respectively. In these experiments,
242 whatever the volume used for contact (200 or 300 µL), no significant difference on the adhesion
243 scores was observed for each strain (P>0.05).

244 To investigate whether the alteration of the cell envelope and adhesion ability of the
245 isogenic mutant could interfere with the cell cytotoxicity, we performed, as shown on Fig. 5,
246 assays measuring the cytotoxicity of the WT and that of the Δ*pnpA* mutant against eukaryotic
247 Caco-2 cells. These data confirmed those reported in our previous reports (Caly et al., 2017;
248 Ladjouzi et al., 2020b). Thus, *E. faecalis* 14 WT is not cytotoxic towards eukaryotic Caco-2 cells,
249 as a survival rate of 85.32% was registered after 24 h of contact (Fig. 5). In the absence of
250 PNPase activity, the viability of Caco-2 cells has not significantly changed (P=0.65) as 88.24%
251 of strains were still viable after 24 hours (Fig. 5). These data underpinned a highly adhesion
252 capability of the mutant Δ*pnpA* without interfering on the cell cytotoxicity.

253

254 **3.3. *E. faecalis* deficient in PNPase activity is highly proteolytic**

255 The proteolytic activity of the WT and Δ*pnpA* mutant was determined to see whether
256 PNPase is involved in such function. Therefore, after 72 h of growth, the Δ*pnpA* mutant
257 underpinned intense zones of proteolysis, compared with WT strain (Fig. 6), indicating a putative
258 interaction between PNPase and synthesis of extracellular proteases in *E. faecalis* 14.

259

260

261

3.4. Transcriptomic analysis revealed a network of deregulated genes

To explain the particular behavior of the Δ*pnpA* mutant obtained from *E. faecalis* 14, we performed a global comparative transcriptomic analysis using total RNA isolated from both strains, after 3 h and 6 h of growth in GM17 medium, under semi-aerobic conditions. As depicted on Fig. 7, a total of 244 differently expressed genes (DEGs) were obtained for the *ΔpnpA* mutant strain (Table S1). An early deregulation permitted to observe that only after 3 h of growth, expression of 39 genes was up-regulated and that of 16 genes was down-regulated. Nonetheless, after 6 h of growth, the number of DEGs has augmented as 201 genes were up-regulated and only 42 down-regulated (Fig. 7). In light to that, important groups of genes as those involved in different cellular mechanisms resulted to be deregulated in the mutant Δ*pnpA*, which argue on the pleiotropic role of PNPase (Table S1). In regard to that, we found 186 DEGs; among which 18 were related to stress responses, 94 to different metabolic pathways, 5 to general cell functions and regulations as signal transduction, 36 to translation, 13 to transport, 11 to DNA replication and repair and 2 to other unclassified functions. Moreover, as indicated in Fig. 8, 27 DEGs were found involved in the cell envelope modifications, in particular in the cell wall structure (23 genes), and 4 in the capsule or membrane structure. Notably, 18 other DEGs were related to the bacterial adhesion and biofilm formation (16 genes) and to the proteolysis (2 genes). These collected transcriptomic data are insightful and could partly explain discrepancies in the phenotypes obtained for the Δ*pnpA* mutant, especially functions related to bacterial cell wall alterations, cell adhesion and proteolytic activity.

4. Discussion

mRNA and protein levels are well-regulated in order to continuously satisfy cellular needs. Post-transcriptional regulation relies mRNA stability and protein turnover and modulates the efficiency of mRNA translation into protein. It has become evident that mRNA degradation is a key checkpoint in the hierarchical of regulatory events, and could therefore help to better understand and decrypt global cell response to different environmental growth conditions.

In general, mRNA degradation in degradosome of Gram-positive bacteria is initiated by endoribonucleolytic cleavage usually attributed to endoribonuclease Y (RNase Y) leading to 3' tails which are then processed by 3'-5' exoribonucleases, among which PNPAse (Cho, 2017).

As above-mentioned, PNPase is an ancient 3'-5'exoribonuclease well conserved in both Gram-negative and Gram-positive bacteria. This enzyme has a role in maintaining RNA levels in the cell (Lin-Chao et al., 2007), and also in the mechanisms of RNA processing and degradation (Cameron et al., 2018). Further roles in mRNA homeostasis, tRNA processing and degradation were previously ascribed to PNPase (Li and Deutscher, 1994), supporting thus the idea that this enzyme has a major role in the biology of the bacterial cell.

In this work, we establish that the absence of PNPase in *E. faecalis* 14, an isolate from meconium (Al Atya et al., 2015) is characterized by atypical phenotypes suggesting a direct or indirect implication of this 3'-5' exoribonuclease. Briefly, in the Δ*pnpA* mutant, we establish a set of modifications, among which clear alteration of the cell-envelope, a high ability of adhesion to Caco-2 eukaryotic cells as well as an enhanced proteolytic activity compared with the WT strain. Further, absence of PNPase seems to have effects on the colony and cell sizes, and cells-organization. Indeed, the Δ*pnpA* mutant cells resulted to be smaller in size than those of the WT

306 strain and organized differently than those of the WT strain which are well known as rugby ball.
307 The Δ*pnpA* mutant exhibited a better adhesion to Caco-2 cells, without having a toxic effect, and
308 showed as well a better proteolytic activity than the WT strain. All these functions are thought to
309 be directly or indirectly associated with PNPase activity.

310 In this study we also performed a transcriptomic study exploring RNAs isolated from both
311 strains after 3 and 6 h of their growths. A set of genes appeared to be down regulated in the
312 Δ*pnpA* mutant and this includes genes associated with transduction, translation, transport, DNA
313 replication, DNA repair, certain metabolic pathways, stress responses, adhesion and biofilm
314 formation, competence and conjugative transfer and other genes related to pathogenesis (See
315 Table S1). In light of this, PNPase was shown to play a role in RNA processing and maturation
316 by modulating the global transcriptome of bacteria like *B. subtilis* and *E. coli.* In direct line,
317 Spanka et al (2021) showed that PNPase can affect the physiology, growth, pigmentation and
318 adaptation of *Rhodobacter sphaeroides* (Spanka et al., 2021). Of note, in *E. coli* a myriad of
319 functions involving a direct or indirect role of PNPase were reported in the literature. These
320 functions include resistance to oxidative stress, UV radiation, and cold acclimation by degrading
321 a large amount of cold shock proteins, transcripts after the cold shock induction (Bonnin and
322 Bouloc, 2015; Rath et al., 2012; Wu et al., 2009), biofilm formation through repression of poly-
323 N-acetylglucosamine (PNAG) (Carzaniga et al., 2012). Furthermore, PNPase activity was also
324 shown to be related to pathogenicity and virulence in Gram-positive and Gram-negative bacteria
325 (Casinhas et al., 2018; Haddad et al., 2009; Numata et al., 2014; Rosenzweig and Chopra, 2013;
326 Sinha et al., 2021).

We will now extend this spectrum of functions involving direct or indirect intervention of PNPase to other bacterial models, including Gram-positive bacteria like *B. subtilis,* in which most of the studies on mRNA stability and characterization of ribonucleases were performed.

In this bacterium, the PNPase would be involved, at least with DNA repair (Cardenas et al., 2009), and cellular competence (Luttinger et al., 1996). Concerning other Gram-positive bacteria, there is the case of *Lactobacillus*; a genus belonging to the group of lactic bacteria. In fact, the authors Reniero et al (1992) reported a high frequency of aggregation promoting factor (APF)-mediated and conjugative in *Lactobacillus* (Reniero et al., 1992). Interestingly, this factor was highlighted in our transcriptomic study as being over expressed in the Δ*pnpA* mutant (Table S1). Similarly, the functions elicited in the literature and presented as having a direct or indirect link with PNPase in Gram-negative and Gram-positive bacteria, also emerge in our transcriptomic study, as being deregulated by the absence of PNPase (Table S1). Of note, our transcriptomic study revealed in the Δ*pnpA* mutant no less than 27 up-regulated genes involved in cell envelope synthesis (Table S1 and Fig.8), which may explain in part the phenotypes observed in the Δ*pnpA* mutant, which is distinguished by an altered cell envelope, reduced cell size, and unusual cell arrangement (Fig.3). The exploitation of the data from this transcriptomic study also revealed, in the Δ*pnpA* mutant, the up-regulation of the *apf* gene coding for the synthesis of the APF protein, whose overproduction causes a drastic alteration of the cell envelope in *Lactobacillus gasseri* 4B2 (Jankovic et al., 2003). This transcriptomic study also revealed a cluster of 16 DEGs involved in adhesion functions and biofilm formation, which could be responsible for the adhesion scores found in the Δ*pnpA* mutant strain (Fig.4).

In the table S1, a group of genes related to the biofilm formation network was found to be strongly up-regulated in the Δ*pnpA* mutant. This group contains the accessory regulator AgrBfs

protein, which is involved in the quorum sensing system signal and controls the expression of the virulence factors in *S. aureus* (Zhang et al., 2002). It is noteworthy that gene coding for APF was as well found to be early up-regulated. The APF protein is involved in the conjugation and autoaggregation (Reniero et al., 1992). Remarkably, in the same group of DEGs, there are genes coding for sortase A and cell wall surface anchor family proteins known for their key roles in many infectious diseases (Gaspar et al., 2005; Lalioui et al., 2005). Of note, activation of manganese ABC transporters enables ion import leading to adherence to extracellular matrix (Fenno et al., 1989). Further, other DEGs gathered within this same functional group like those involved in the cell division, complete the molecular biofilm formation network.

As depicted on Fig.8, two DEGs were connected to proteolysis processes that were early up-regulated. Thus, the gene coding for a zinc metalloproteinase precursor was up-regulated at 3h and became strongly up-regulated at 6h in the Δ*pnpA* mutant strain. Overall, zinc metalloproteases belong to microbial proteases, which are predominantly extracellular involved in the virulence (Häse and Finkelstein, 1993). Similarly, an up-regulation was observed for the gene coding for a serine proteinase of V8 family performing proteinase activity (Dancer et al., 1990). Another early-regulated gene was that coding for an extracellular protein, suggesting that the Δ*pnpA* mutant strain increases several biotic and/or abiotic interactions (Dalbey and Kuhn, 2012), probably involved in defense or virulence functions (Lee and Schneewind, 2001; Ma and Guttman, 2008). Taken together, these up-regulated proteinases could explain the enhanced proteolytic activity observed for the Δ*pnpA* mutant strain (Fig.6). Indeed, PNPase was reported to be important in the regulation of small RNAs that control the outer membrane proteins expression (Andrade and Arraiano, 2008).

It was reported that ribonuclease J1 is essential in *E. facalis* (Salze et al., 2020). In this transcriptomic study, we observed that the gene encoding this enzyme is overexpressed in the mutant after 6 hours of growth, most likely indicating a compensatory effect to compensate for the absence of PNPase. Autoregulation of RNase gene expression exploit enzymatic activity and act at the level of mRNA stability in a Gram-positive bacterium (Condon and Bechhofer, 2011), and presumably, the same mechanism is occurring in *E. faecalis* 14.

5. Conclusion

In this study, we constructed a mutant deficient in PNPase synthesis in *E. faecalis* 14; a strain formerly isolated from meconium. The transcriptomic study enabled first snapshot on the genes or the network of genes that are deregulated in the absence of the PNPase. However, from a physiological point of view, it is clear that the absence of this major 3'-5' exoribonuclease has an impact on the physiology and cellular structure of the bacterium. In addition to the alteration of the cell envelope, we have highlighted the reduced size of the cells and colonies in the Δ*pnpA* mutant strain than in the WT strain. Similarly, the Δ*pnpA* mutant strain has a high proteolytic activity and a better ability to adhere to Caco2 cells than the WT. Therefore, all these observed effects involve directly or indirectly the PNPase activity in *E. faecalis* 14.

Conflict of interest: The authors declare no competing interests

Author contributions: Conceptualization and experiment design: DD, RL, MD and ADL. RL and MD performed the experiments and ADL carried out the transcriptomic analysis. DD, RL, MD and ADL revised and approved the manuscript dissertation. DD obtained the financial supported for this project.

Funding: This work was funded by the CPER/FEDER grant allocated by la Région des Hauts-de-France (2016-2021).

Acknowledgments: We would like to thank Loïc Brunet and Anne-Sophie Lacoste of the BICeL-University of Lille for their technical assistance. The TEM observations were performed on device of the BICeL-Campus CS core facility acquired through a funding from the Agence Nationale de la Recherche, ANR (10EQPX-04-01). The authors are grateful to Rezak Mendil for assistance in cell cytotoxicity and cell adhesion assays. The authors would like to thank Dr. Steve W. Elson for reading and improving the English of the manuscript.

References

Al Atya, A.K., Drider-Hadiouche, K., Ravallec, R., Silvain, A., Vachee, A., Drider, D., 2015. Probiotic potential of *Enterococcus faecalis* strains isolated from meconium. Front Microbiol 6. https://doi.org/10.3389/fmicb.2015.00227

Andrade, J.M., Arraiano, C.M., 2008. PNPase is a key player in the regulation of small RNAs that control the expression of outer membrane proteins. RNA 14, 543–551. https://doi.org/10.1261/rna.683308

Arraiano, C.M., Andrade, J.M., Domingues, S., Guinote, I.B., Malecki, M., Matos, R.G., Moreira, R.N., Pobre, V., Reis, F.P., Saramago, M., Silva, I.J., Viegas, S.C., 2010. The critical role of RNA processing and degradation in the control of gene expression. FEMS Microbiol Rev 34, 883–923. https://doi.org/10.1111/j.1574-6976.2010.00242.x

Becket, E., Tse, L., Yung, M., Cosico, A., Miller, J.H., 2012. Polynucleotide phosphorylase plays an important role in the generation of spontaneous mutations in *Escherichia coli*. J Bacteriol 194, 5613–5620. https://doi.org/10.1128/JB.00962-12

Bendali, F., Durand, A., Hébraud, M., Sadoun, D., 2011. *Lactobacillus paracasei* subsp. paracasei, an Algerian isolate with antibacterial activity against enteric pathogens and probiotic fitness. J. Food Nutr. Res. 50, 139–149.

Bonnin, R.A., Bouloc, P., 2015. RNA Degradation in *Staphylococcus aureus*: Diversity of ribonucleases and their impact. Int J Genomics 2015, 395753. https://doi.org/10.1155/2015/395753

Broglia, L., Lécrivain, A.-L., Renault, T.T., Hahnke, K., Ahmed-Begrich, R., Le Rhun, A., Charpentier, E., 2020. An RNA-seq based comparative approach reveals the transcriptome-wide interplay between 3′-to-5′ exoRNases and RNase Y. Nat Commun 11, 1587. https://doi.org/10.1038/s41467-020-15387-6

427 Bryan, E.M., Bae, T., Kleerebezem, M., Dunny, G.M., 2000. Improved vectors for nisin-
428 controlled expression in Gram-positive bacteria. Plasmid 44, 183–190.
429 https://doi.org/10.1006/plas.2000.1484
430 Caly, D.L., Chevalier, M., Flahaut, C., Cudennec, B., Al Atya, A.K., Chataigné, G., D'Inca, R.,
431 Auclair, E., Drider, D., 2017. The safe enterocin DD14 is a leaderless two-peptide
432 bacteriocin with anti-*Clostridium perfringens* activity. Int. J. Antimicrob. Agents 49, 282–
433 289. https://doi.org/10.1016/j.ijantimicag.2016.11.016
434 Cameron, T.A., Matz, L.M., Lay, N.R.D., 2018. Polynucleotide phosphorylase: Not merely an
435 RNase but a pivotal post-transcriptional regulator. PLOS Genetics 14, e1007654.
436 https://doi.org/10.1371/journal.pgen.1007654
437 Cardenas, P.P., Carrasco, B., Sanchez, H., Deikus, G., Bechhofer, D.H., Alonso, J.C., 2009.
438 *Bacillus subtilis* polynucleotide phosphorylase 3'-to-5' DNase activity is involved in
439 DNA repair. Nucleic Acids Res 37, 4157–4169. https://doi.org/10.1093/nar/gkp314
440 Cardenas, P.P., Carzaniga, T., Zangrossi, S., Briani, F., Garcia-Tirado, E., Dehò, G., Alonso, J.C.,
441 2011. Polynucleotide phosphorylase exonuclease and polymerase activities on single-
442 stranded DNA ends are modulated by RecN, SsbA and RecA proteins. Nucleic Acids Res
443 39, 9250–9261. https://doi.org/10.1093/nar/gkr635
444 Carzaniga, T., Antoniani, D., Dehò, G., Briani, F., Landini, P., 2012. The RNA processing
445 enzyme polynucleotide phosphorylase negatively controls biofilm formation by
446 repressing poly-N-acetylglucosamine (PNAG) production in Escherichia coli C. BMC
447 Microbiol 12, 270. https://doi.org/10.1186/1471-2180-12-270
448 Cascante-Estepa, N., Gunka, K., Stülke, J., 2016. Localization of components of the RNA-
449 degrading machine in *Bacillus subtilis*. Front Microbiol 7, 1492.
450 https://doi.org/10.3389/fmicb.2016.01492
451 Casinhas, J., Matos, R.G., Haddad, N., Arraiano, C.M., 2018. Biochemical characterization of
452 *Campylobacter jejuni* PNPase, an exoribonuclease important for bacterial pathogenicity.
453 Biochimie 147, 70–79. https://doi.org/10.1016/j.biochi.2018.01.001
454 Cho, K.H., 2017. The structure and function of the Gram-positive bacterial RNA degradosome.
455 Front Microbiol 8, 154. https://doi.org/10.3389/fmicb.2017.00154
456 Condon, C., Bechhofer, D.H., 2011. Regulated RNA stability in the Gram positives. Curr. Opin.
457 Microbiol. 14, 148–154. https://doi.org/10.1016/j.mib.2011.01.010
458 Dalbey, R.E., Kuhn, A., 2012. Protein Traffic in Gram-negative bacteria – how exported and
459 secreted proteins find their way. FEMS Microbiology Reviews 36, 1023–1045.
460 https://doi.org/10.1111/j.1574-6976.2012.00327.x
461 Dancer, S.J., Garratt, R., Saldanha, J., Jhoti, H., Evans, R., 1990. The epidermolytic toxins are
462 serine proteases. FEBS Lett 268, 129–132. https://doi.org/10.1016/0014-5793(90)80990-z
463 de Albuquerque, T.M.R., Garcia, E.F., de Oliveira Araújo, A., Magnani, M., Saarela, M., de
464 Souza, E.L., 2018. In vitro characterization of *Lactobacillus* strains isolated from fruit
465 processing by-products as potential probiotics. Probiotics Antimicrob Proteins 10, 704–
466 716. https://doi.org/10.1007/s12602-017-9318-2
467 Fenno, J.C., LeBlanc, D.J., Fives-Taylor, P., 1989. Nucleotide sequence analysis of a type 1
468 fimbrial gene of *Streptococcus sanguis* FW213. Infect Immun 57, 3527–3533.
469 https://doi.org/10.1128/iai.57.11.3527-3533.1989

Gao, P., Pinkston, K.L., Bourgogne, A., Murray, B.E., Hoof, A. van, Harvey, B.R., 2017. Functional studies of *E. faecalis* RNase J2 and its role in virulence and fitness. PLOS ONE 12, e0175212. https://doi.org/10.1371/journal.pone.0175212

Gaspar, A.H., Marraffini, L.A., Glass, E.M., DeBord, K.L., Ton-That, H., Schneewind, O., 2005. *Bacillus anthracis* sortase A (SrtA) anchors LPXTG motif-containing surface proteins to the cell wall envelope. J Bacteriol 187, 4646–4655. https://doi.org/10.1128/JB.187.13.4646-4655.2005

Haddad, N., Burns, C.M., Bolla, J.M., Prévost, H., Fédérighi, M., Drider, D., Cappelier, J.M., 2009. Long-term survival of *Campylobacter jejuni* at low temperatures is dependent on polynucleotide phosphorylase activity. Appl Environ Microbiol 75, 7310–7318. https://doi.org/10.1128/AEM.01366-09

Häse, C.C., Finkelstein, R.A., 1993. Bacterial extracellular zinc-containing metalloproteases. Microbiol Rev 57, 823–837. https://doi.org/10.1128/mr.57.4.823-837.1993

Jankovic, I., Ventura, M., Meylan, V., Rouvet, M., Elli, M., Zink, R., 2003. Contribution of aggregation-promoting factor to maintenance of cell shape in *Lactobacillus gasseri* 4B2. J Bacteriol 185, 3288–3296. https://doi.org/10.1128/JB.185.11.3288-3296.2003

Ladjouzi, R., Lucau-Danila, A., Benachour, A., Drider, D., 2020a. A leaderless two-peptide bacteriocin, enterocin DD14, is involved in its own self-immunity: Evidence and insights. Front Bioeng Biotechnol 8, 644. https://doi.org/10.3389/fbioe.2020.00644

Ladjouzi, R., Lucau-Danila, A., Drider, D., 2020b. Metabolic shift of an isogenic strain of *Enterococcus faecalis* 14, deficient in its own bacteriocin synthesis, as revealed by a transcriptomic analysis. International Journal of Molecular Sciences 21, 4653. https://doi.org/10.3390/ijms21134653

Lalioui, L., Pellegrini, E., Dramsi, S., Baptista, M., Bourgeois, N., Doucet-Populaire, F., Rusniok, C., Zouine, M., Glaser, P., Kunst, F., Poyart, C., Trieu-Cuot, P., 2005. The SrtA Sortase of *Streptococcus agalactiae* is required for cell wall anchoring of proteins containing the LPXTG motif, for adhesion to epithelial cells, and for colonization of the mouse intestine. Infect Immun 73, 3342–3350. https://doi.org/10.1128/IAI.73.6.3342-3350.2005

Lécrivain, A.-L., Le Rhun, A., Renault, T.T., Ahmed-Begrich, R., Hahnke, K., Charpentier, E., 2018. In vivo 3'-to-5' exoribonuclease targetomes of *Streptococcus pyogenes*. Proc Natl Acad Sci U S A 115, 11814–11819. https://doi.org/10.1073/pnas.1809663115

Lee, V.T., Schneewind, O., 2001. Protein secretion and the pathogenesis of bacterial infections. Genes Dev 15, 1725–1752. https://doi.org/10.1101/gad.896801

Lehnik-Habrink, M., Lewis, R.J., Mäder, U., Stülke, J., 2012. RNA degradation in *Bacillus subtilis*: an interplay of essential endo- and exoribonucleases. Mol Microbiol 84, 1005–1017. https://doi.org/10.1111/j.1365-2958.2012.08072.x

Leszczyniecka, M., DeSalle, R., Kang, D., Fisher, P.B., 2004. The origin of polynucleotide phosphorylase domains. Molecular Phylogenetics and Evolution 31, 123–130. https://doi.org/10.1016/j.ympev.2003.07.012

Li, Z., Deutscher, M.P., 1994. The role of individual exoribonucleases in processing at the 3' end of *Escherichia coli* tRNA precursors. J Biol Chem 269, 6064–6071.

Lin-Chao, S., Chiou, N.-T., Schuster, G., 2007. The PNPase, exosome and RNA helicases as the building components of evolutionarily-conserved RNA degradation machines. J Biomed Sci 14, 523–532. https://doi.org/10.1007/s11373-007-9178-y

514 Luttinger, A., Hahn, J., Dubnau, D., 1996. Polynucleotide phosphorylase is necessary for
515 competence development in *Bacillus subtilis*. Mol Microbiol 19, 343–356.
516 https://doi.org/10.1046/j.1365-2958.1996.380907.x
517 Ma, W., Guttman, D.S., 2008. Evolution of prokaryotic and eukaryotic virulence effectors. Curr
518 Opin Plant Biol 11, 412–419. https://doi.org/10.1016/j.pbi.2008.05.001
519 Mohanty, B.K., Kushner, S.R., 2000. Polynucleotide phosphorylase functions both as a 3′ → 5′
520 exonuclease and a poly(A) polymerase in *Escherichia coli*. PNAS 97, 11966–11971.
521 Numata, S., Nagata, M., Mao, H., Sekimizu, K., Kaito, C., 2014. CvfA protein and
522 polynucleotide phosphorylase act in an opposing manner to regulate *Staphylococcus*
523 *aureus* virulence. J Biol Chem 289, 8420–8431. https://doi.org/10.1074/jbc.M114.554329
524 Pinto, M., Robineleon, S., Appay, M.D., Kedinger, M., Triadou, N., Dussaulx, E., Lacroix, B.,
525 Simonassmann, P., Haffen, K., Fogh, J., Pinto, M., Robine, S., Appay, M.-D., Lacroix, B.,
526 Assmann, P.F., Fogh, J., Appay, M.D., Assman, P.F., Fogh, J., Zweibaum, A., Pinto, L.S.,
527 Appay, M.D., Zwwibaum, A., Robin, S., Simon, P., Robineloeon, S., 1983. Enterocyte-
528 like differentiation and polarization of the human-colon carcinoma cell-line Caco-2 in
529 culture.
530 Rath, D., Mangoli, S.H., Pagedar, A.R., Jawali, N., 2012. Involvement of pnp in survival of UV
531 radiation in *Escherichia coli* K-12. Microbiology 158, 1196–1205.
532 https://doi.org/10.1099/mic.0.056309-0
533 Reniero, R., Cocconcelli, P., Bottazzi, V., Morelli, L., 1992. High frequency of conjugation in
534 *Lactobacillus* mediated by an aggregation-promoting factor. Journal of General
535 Microbiology 138, 763–768. https://doi.org/10.1099/00221287-138-4-763
536 Rosenzweig, J.A., Chopra, A.K., 2013. The exoribonuclease polynucleotide phosphorylase
537 influences the virulence and stress responses of yersiniae and many other pathogens.
538 Front Cell Infect Microbiol 3, 81. https://doi.org/10.3389/fcimb.2013.00081
539 Salvo, E., Alabi, S., Liu, B., Schlessinger, A., Bechhofer, D.H., 2016. Interaction of *Bacillus*
540 *subtilis* Polynucleotide Phosphorylase and RNase Y: structural mapping and effect on
541 mRNA turnover. J Biol Chem 291, 6655–6663. https://doi.org/10.1074/jbc.M115.711044
542 Salze, M., Muller, C., Bernay, B., Hartke, A., Clamens, T., Lesouhaitier, O., Rincé, A., 2020.
543 Study of key RNA metabolism proteins in *Enterococcus faecalis*. RNA Biology 17, 794–
544 804. https://doi.org/10.1080/15476286.2020.1728103
545 Sambrook, J., Russell, D.W., 2001. Molecular Cloning: A Laboratory Manual. Cold Spring
546 Harbor Laboratory Press.
547 Sinha, D., Frick, J.P., Clemons, K., Winkler, M.E., De Lay, N.R., 2021. Pivotal roles for
548 ribonucleases in *Streptococcus pneumoniae* Pathogenesis. mBio 12, e0238521.
549 https://doi.org/10.1128/mBio.02385-21
550 Spanka, D.-T., Reuscher, C.M., Klug, G., 2021. Impact of PNPase on the transcriptome of
551 *Rhodobacter sphaeroides* and its cooperation with RNase III and RNase E. BMC
552 Genomics 22, 106. https://doi.org/10.1186/s12864-021-07409-4
553 Spickler, C., Mackie, G.A., 2000. Action of RNase II and Polynucleotide Phosphorylase against
554 RNAs Containing Stem-Loops of Defined Structure. Journal of Bacteriology 182, 2422–
555 2427. https://doi.org/10.1128/JB.182.9.2422-2427.2000
556 Thurlow, L.R., Thomas, V.C., Hancock, L.E., 2009. Capsular Polysaccharide Production in
557 *Enterococcus faecalis* and contribution of CpsF to capsule serospecificity. J. Bacteriol.
558 191, 6203–6210. https://doi.org/10.1128/JB.00592-09

559 Wu, J., Jiang, Z., Liu, M., Gong, X., Wu, S., Burns, C.M., Li, Z., 2009. Polynucleotide
560 phosphorylase protects *Escherichia coli* against oxidative stress. Biochemistry 48, 2012–
561 2020. https://doi.org/10.1021/bi801752p
562 Wurtmann, E.J., Wolin, S.L., 2009. RNA under attack: cellular handling of RNA damage. Crit
563 Rev Biochem Mol Biol 44, 34–49. https://doi.org/10.1080/10409230802594043
564 Yanisch-Perron, C., Vieira, J., Messing, J., 1985. Improved M13 phage cloning vectors and host
565 strains: nucleotide sequences of the M13mpl8 and pUC19 vectors. Gene 33, 103–119.
566 https://doi.org/10.1016/0378-1119(85)90120-9
567 Zangrossi, S., Briani, F., Ghisotti, D., Regonesi, M.E., Tortora, P., Dehò, G., 2000.
568 Transcriptional and post-transcriptional control of polynucleotide phosphorylase during
569 cold acclimation in *Escherichia coli*. Mol Microbiol 36, 1470–1480.
570 https://doi.org/10.1046/j.1365-2958.2000.01971.x
571 Zhang, L., Gray, L., Novick, R.P., Ji, G., 2002. Transmembrane topology of AgrB, the protein
572 involved in the post-translational modification of AgrD in *Staphylococcus aureus*. J Biol
573 Chem 277, 34736–34742. https://doi.org/10.1074/jbc.M205367200
574

575

576 **Figure legends**

577 **Fig. 1:** Growth curves of *E. faecalis* WT (●), Δ*pnpA* mutant (■) and the Δ*pnpA*-complemented
578 (▲) strains grown in GM17 medium. The standard deviations are presented by vertical bars. The
579 asterisk (*) indicates that the growth rate is significantly different from that of the WT strain
580 using the student test ($p<0.05$).

581 **Fig. 2.** Macroscopic appearance and size of *E. faecalis* WT, Δ*pnpA* mutant and the Δ*pnpA*-
582 complemented colonies on the same BHI agar plate.

583 **Fig. 3.** Transmission electron microscopy (TEM) micrographs of *E. faecalis WT* and its Δ*pnpA*
584 mutant strain. Arrows indicate the main alterations on cell wall of the Δ*pnpA* mutant

585 **Fig. 4.** Adhesion of *E. faecalis WT* and its Δ*pnpA* mutant strains to Caco-2 cells after 2h30 mn
586 of contact. The contact was performed using two volumes 200 µL and 300 µL (6.10^9 cfu.mL-1).
587 The vertical bars represent the standard deviations. The asterisk (*) indicates a significantly
588 different growth rate ($p<0.05$) between the Δ*pnpA* mutant and the WT.

589 **Fig. 5.** Cytotoxic effect of *E. faecalis* 14 WT and its Δ*pnpA* mutant strains on Caco-2 cells after
590 24 h of contact. Three independent experiments were performed and the means of data are
591 represented. Means and standard bars are shown. “ns” denotes: not significant

592 **Fig. 6.** Proteolytic activity of *E. faecalis* 14 WT and its Δ*pnpA* after 72 h of growth on milk
593 agar. A representative profile of three independent experiments is presented.

594 **Fig. 7.** Venn diagram representing the number of up- and down-regulated DEGs in *ΔpnpA* strain
595 of *E. faecalis* at 3h and 6h of culture respectively.

596 **Fig. 8.** Gene expression profiles of DEGs involved in cell envelope modifications and
597 pathogenesis in *ΔpnpA* strain of *E. faecalis*. Log2 FC of individual *ΔpnpA* (P1-P3) vs. mean of

598 WT were represented for 3h and 6h of culture respectively. Functional groups are indicated in
599 the right of the picture.

600 **Table 1.** Bacterial strains and plasmids used in this study.

Designation	Relevant characteristics	Reference
Strain		
Enterococci		
Enterococcus *faecalis* 14	Wild-type strain isolated from meconium	(Al Atya et al., 2015)
14 Δ*pnpA*	*E. faecalis* 14 *pnpA* deletion mutant	This study
14 Δ*pnpA -C*	*E. faecalis* 14Δ *pnpA* harboring pMSP3535:*pnpA* complemented strain	This study
E. coli		
XL-1 Blue	*recA1 endA1 gyrA96 thi-1 hsdR17 supE44 relA1 Lac* [F' *proAB lacI*^{q}ZΔM15Tn*10* (Tet^{R})]	Stratagene
JM109	*recA1. endAl, gyrA96, thi. hsdR17, supE44, relA1, I-, A(iac-proAB), [F', traD36, proAB, iacI^{q}ZAM15]*	(Yanisch-Perron et al., 1985)
Plasmids		
pLT06	*lacZ*, P-*pheS* from pCJK47, *Cm* from pGB354, *orfB*, *orfC*, *repA* (*Ts*), *orfD* from pCASPER	(Thurlow et al., 2009)
pLT06Δ*pnpA*	pLT06 derivative carrying a 1.91 kb DNA fragment from *E. faecalis* 14 harboring mutated *pnpA* gene	This study
pMSP3535	Em^{R}, *nis*R, *nis*K P*nis*A (nisin-inducible promoter)	(Bryan et al., 2000)
pMSP3535:*pnpA*	pMSP3535 derivative carrying a 2.36 kb DNA fragment from *E.faecalis* 14 with *pnpA* gene	This study
pGEM-t Easy	Ap^{R} cloning vector	Promega
pGEM-t EasyΔ*pnpA*	pGEM-t Easy derivative carrying a 1.91 kb DNA fragment from *E. faecalis* 14 harboring mutated *pnpA* gene	This study

601 *Em*, erythromycin; *Ap, ampicillin; Tet*, tetracycline; *Cm*, chloramphenicol; *bgaB*, Beta-galactosidase; R,
602 resistant; S, sensitive; *Ts*, thermosensitive; *nis*, nisin

603 **Table 2.** Oligonucleotides used in this study.

Name	Sequence 5'-------->3'	The use for
pnpA-1F	ACCCTCGAGTTCAATGCGGACAACTTTTG	amplification of *pnpA* up-stream fragment
pnpA-2R	CCAACGTTTAGGATTACGTCGCGGATGGCCGTAAATTAGAC	
pnpA-3F	GTCTAATTTACGGCCATCCGCGACGTAATCCTAAACGTTGG	amplification of *pnpA* down-stream fragment
pnpA-4R	TGTGAATTCCGCCAGCCATGTCAAAATA	
pnpA-5F	GCGCAAATACTTGCTTGTGA	Internal primers; verification of the plasmid integration
pnpA-6R	AAATCGGTCACCGTCGTAAC	
pnpA-7F	ATGGATCAAGCCATCTTTGC	External primers, screening of the mutants
pnpA-8R	AAAAAGTGGCCACAATGGTC	
pnpA-CompF (*Pst* I)	ATTAAACTGCAGGGAAGCTTCCTTGGTTTTCG	Complementation of Δ*pnpA* mutant
pnpA-CompR (*BamH*I)	ATTAAAGGATCCGAGCAGCAACGACTTGTTAC	
PU	GTAAAACGACGGCCAGT	Cloning verification in pGEM-t Easy plasmid
PR	CAGGAAACAGCTATGAC	
PMSP3535-F	GATACAATGATTTCGTTCGAAGG	Cloning verification in pMSM3535 plasmid
PMSP3535-R	GCTTATCGAAATTAATACGACTCAC	
ORIf	CAATAATCGCATCCGATTGCA	Cloning verification in pLT06 plasmid
KS05seqR	CCTATTATACCATATTTTGGAC	

604 *Underlined sequences correspond to the recognition sites of the restriction endonucleases mentioned in
605 brackets in the primer name.
606

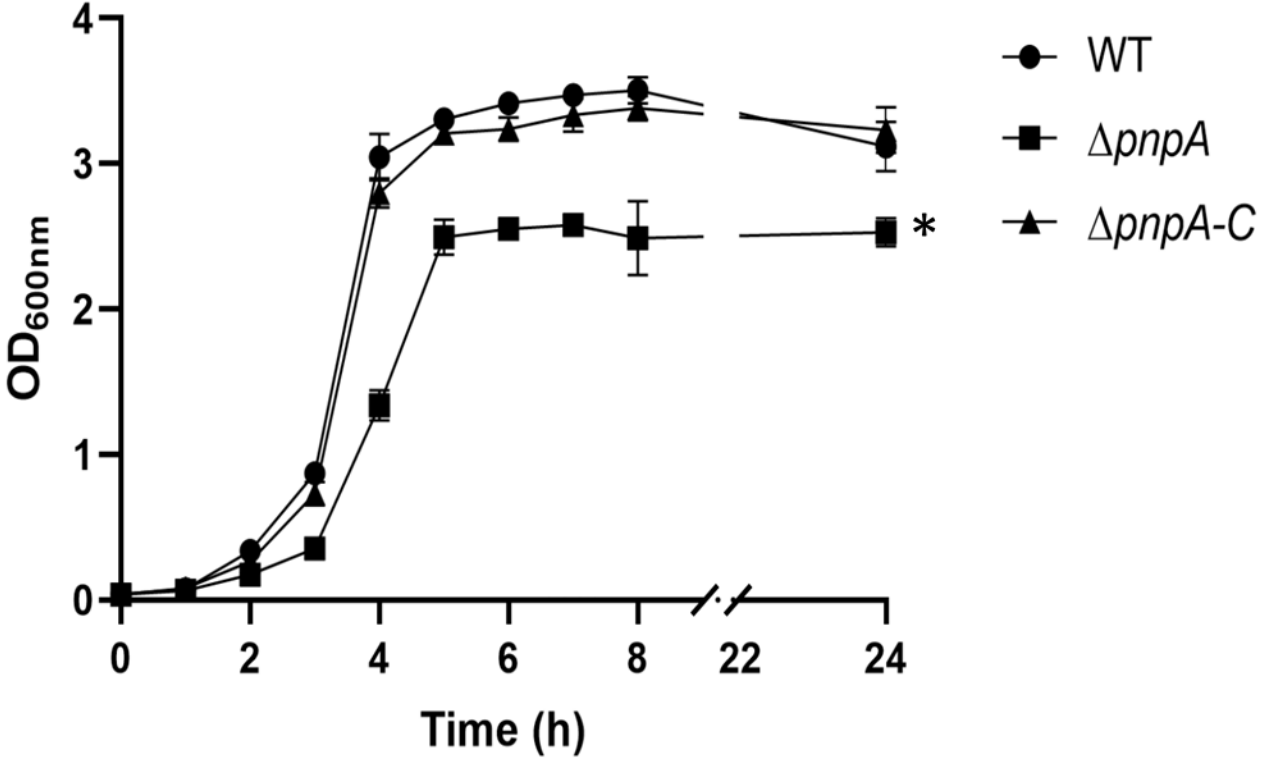
4
3
2
1
0
OD600nm
0
2
4
6
8
22
24
Time (h)
*
WT
ΔpnpA
ΔpnpA-C

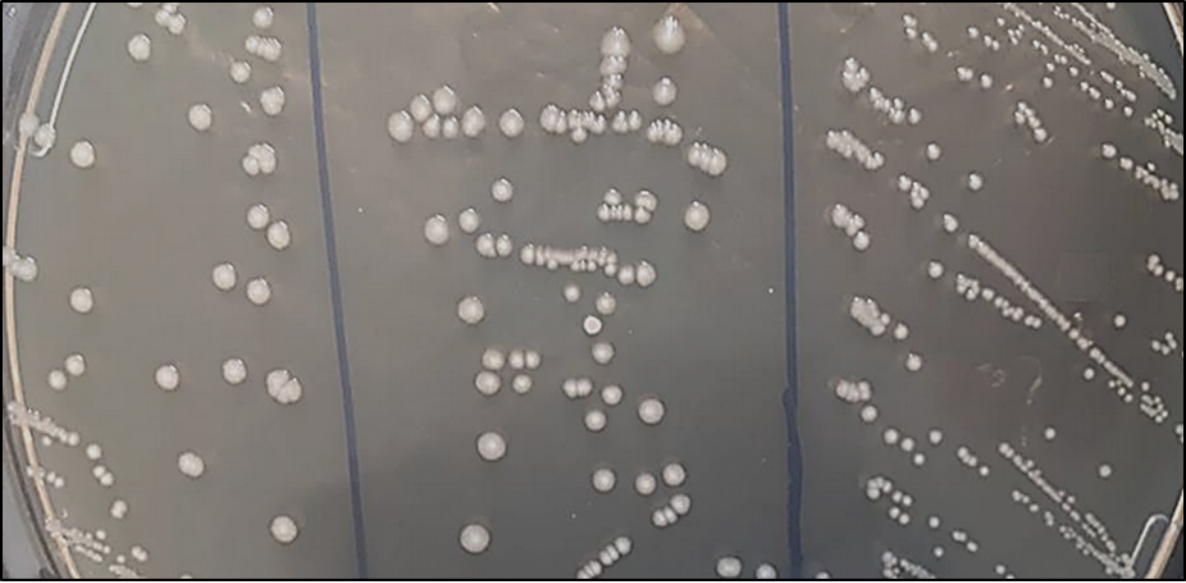
WT
ΔpnpA-C
ΔpnpA

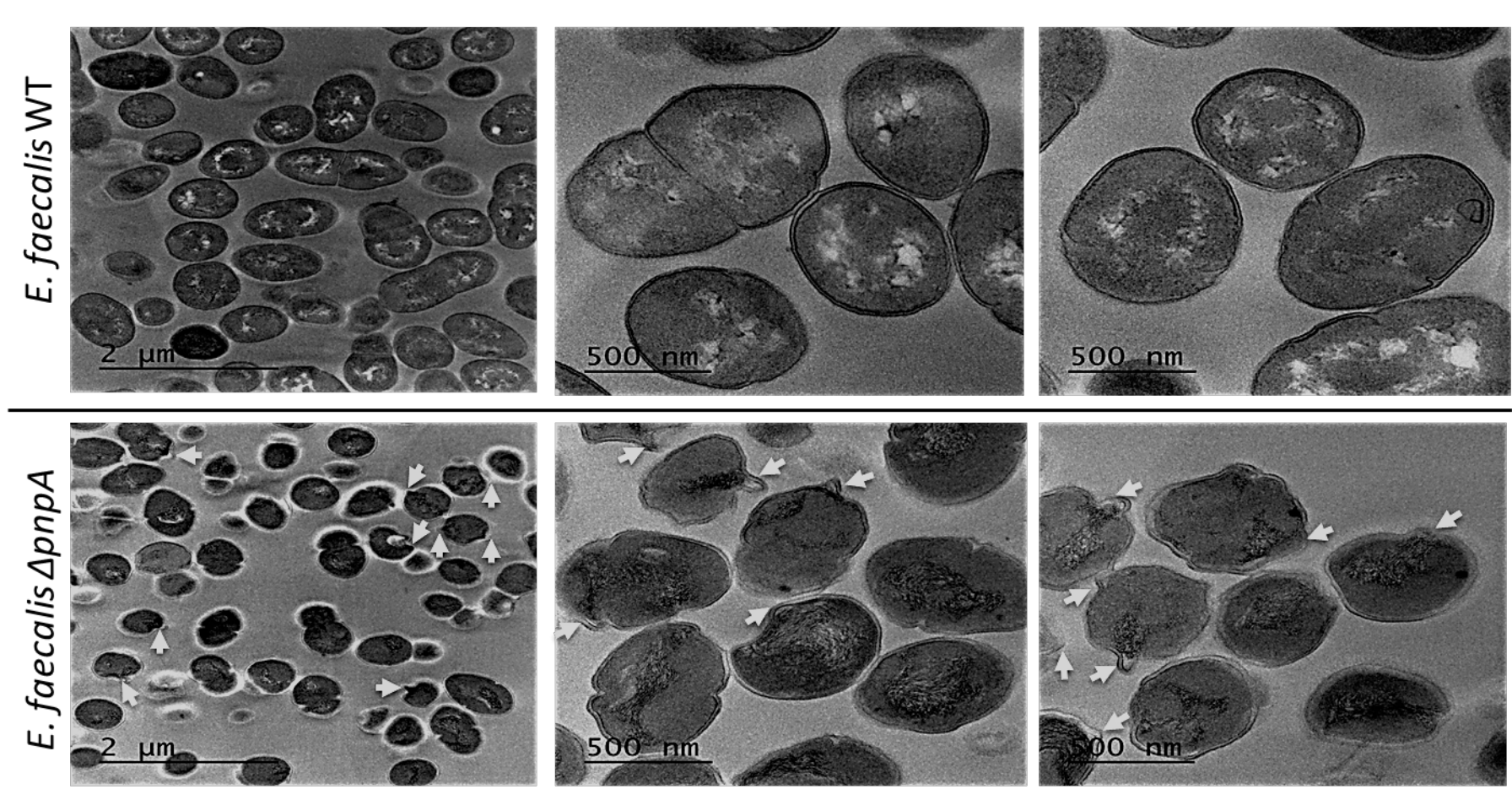
E. faecalis WT
2 µm
500 nm
500 nm
E. faecalis ΔpnpA
2 µm
500 nm
500 nm

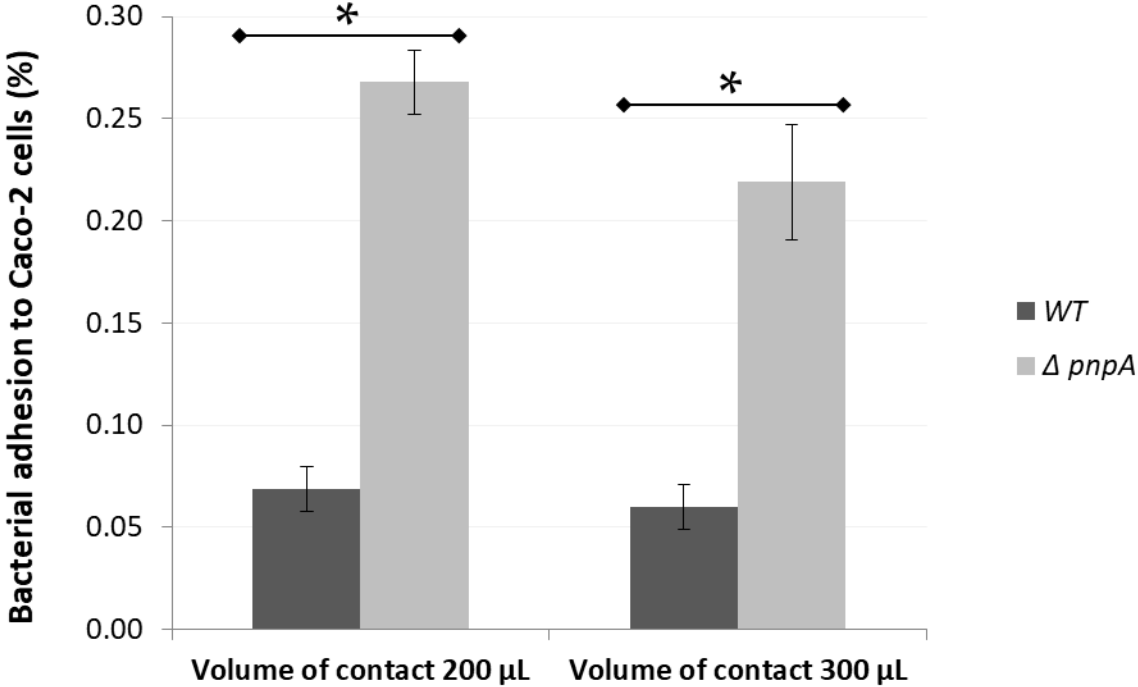
Bacterial adhesion to Caco-2 cells (%)
0.30
0.25
0.20
0.15
0.10
0.05
0.00
*
*
Volume of contact 200 µL
Volume of contact 300 µL
WT
Δ pnpA

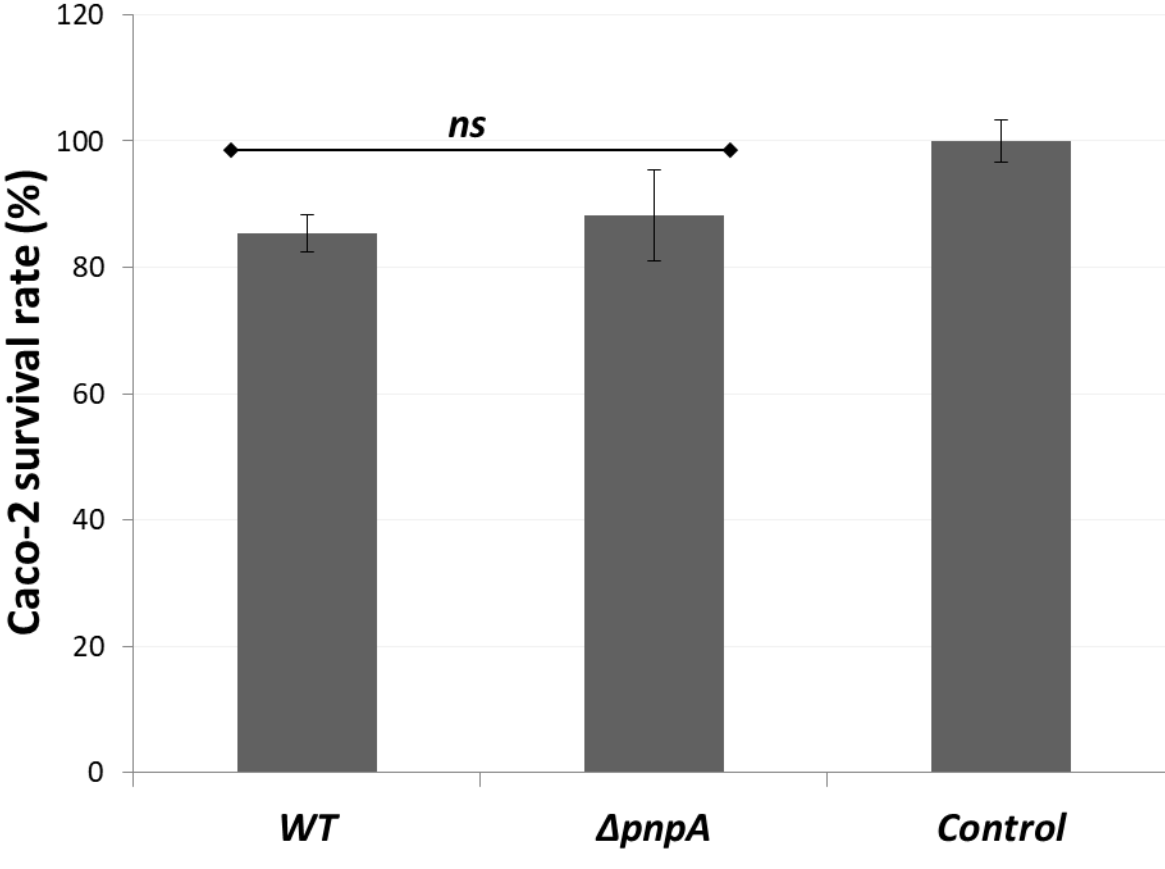
120
100
80
60
40
20
0
Caco-2 survival rate (%)
ns
WT
ΔpnpA
Control

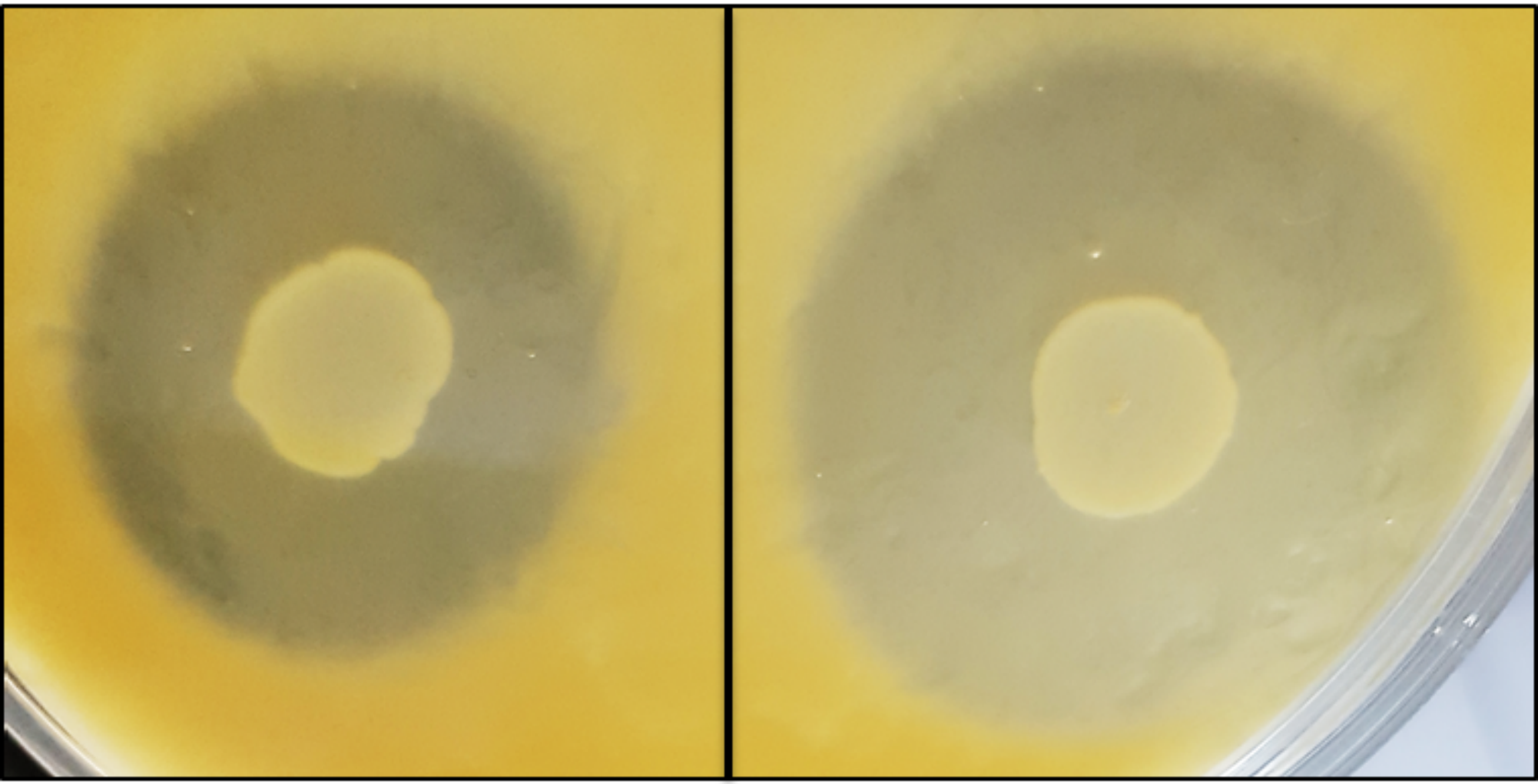
WT
ΔpnpA

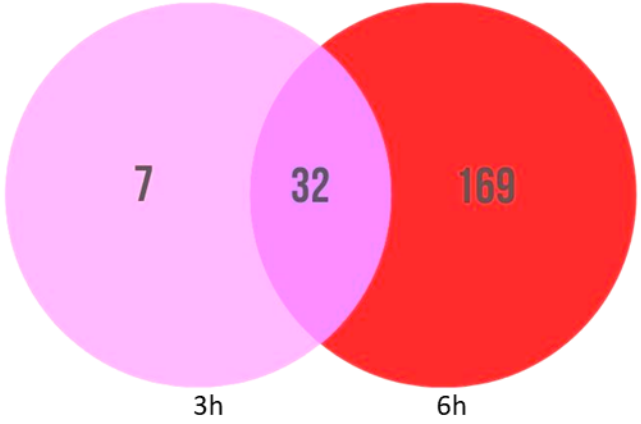

Up-regulated genes

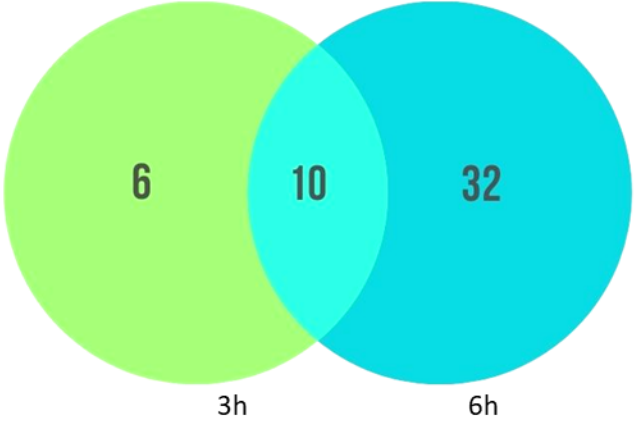

Down-regulated genes

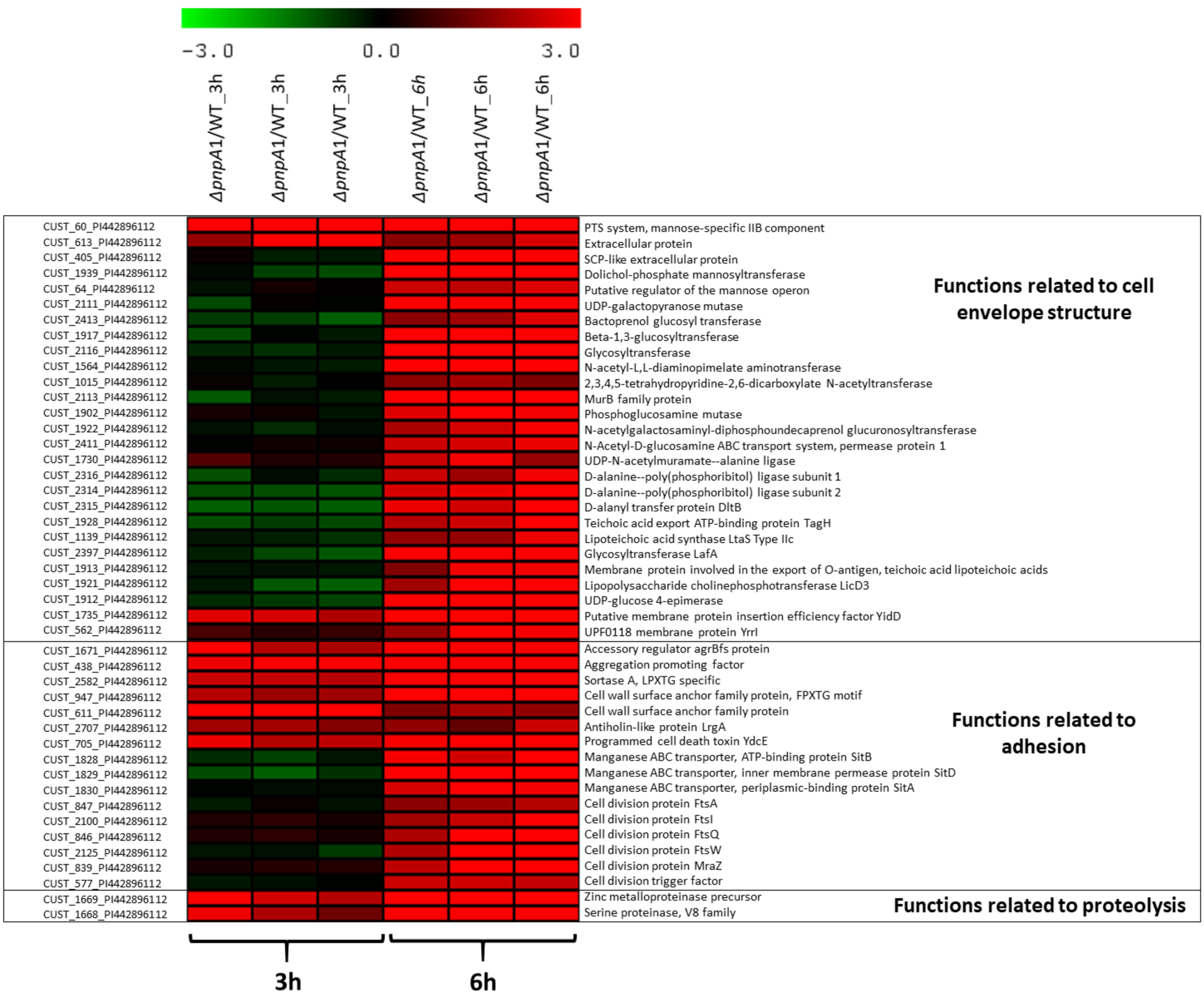
-3.0
0.0
3.0
ΔpnpA1/WT_3h
ΔpnpA1/WT_3h
ΔpnpA1/WT_3h
ΔpnpA1/WT_6h
ΔpnpA1/WT_6h
ΔpnpA1/WT_6h
CUST_60_PI442896112 PTS system, mannose-specific IIB component
CUST_613_PI442896112 Extracellular protein
CUST_405_PI442896112 SCP-like extracellular protein
CUST_1939_PI442896112 Dolichol-phosphate mannosyltransferase
CUST_64_PI442896112 Putative regulator of the mannose operon
CUST_2111_PI442896112 UDP-galactopyranose mutase
CUST_2413_PI442896112 Bactoprenol glucosyl transferase
CUST_1917_PI442896112 Beta-1,3-glucosyltransferase
CUST_2116_PI442896112 Glycosyltransferase
CUST_1564_PI442896112 N-acetyl-L,L-diaminopimelate aminotransferase
CUST_1015_PI442896112 2,3,4,5-tetrahydropyridine-2,6-dicarboxylate N-acetyltransferase
CUST_2113_PI442896112 MurB family protein
CUST_1902_PI442896112 Phosphoglucosamine mutase
CUST_1922_PI442896112 N-acetylgalactosaminyl-diphosphoundecaprenol glucuronosyltransferase
CUST_2411_PI442896112 N-Acetyl-D-glucosamine ABC transport system, permease protein 1
CUST_1730_PI442896112 UDP-N-acetylmuramate--alanine ligase
CUST_2316_PI442896112 D-alanine--poly(phosphoribitol) ligase subunit 1
CUST_2314_PI442896112 D-alanine--poly(phosphoribitol) ligase subunit 2
CUST_2315_PI442896112 D-alanyl transfer protein DltB
CUST_1928_PI442896112 Teichoic acid export ATP-binding protein TagH
CUST_1139_PI442896112 Lipoteichoic acid synthase LtaS Type IIc
CUST_2397_PI442896112 Glycosyltransferase LafA
CUST_1913_PI442896112 Membrane protein involved in the export of O-antigen, teichoic acid lipoteichoic acids
CUST_1921_PI442896112 Lipopolysaccharide cholinephosphotransferase LicD3
CUST_1912_PI442896112 UDP-glucose 4-epimerase
CUST_1735_PI442896112 Putative membrane protein insertion efficiency factor YidD
CUST_562_PI442896112 UPF0118 membrane protein YrrI
Functions related to cell envelope structure
CUST_1671_PI442896112 Accessory regulator agrBfs protein
CUST_438_PI442896112 Aggregation promoting factor
CUST_2582_PI442896112 Sortase A, LPXTG specific
CUST_947_PI442896112 Cell wall surface anchor family protein, FPXTG motif
CUST_611_PI442896112 Cell wall surface anchor family protein
CUST_2707_PI442896112 Antiholin-like protein LrgA
CUST_705_PI442896112 Programmed cell death toxin YdcE
CUST_1828_PI442896112 Manganese ABC transporter, ATP-binding protein SitB
CUST_1829_PI442896112 Manganese ABC transporter, inner membrane permease protein SitD
CUST_1830_PI442896112 Manganese ABC transporter, periplasmic-binding protein SitA
CUST_847_PI442896112 Cell division protein FtsA
CUST_2100_PI442896112 Cell division protein FtsI
CUST_846_PI442896112 Cell division protein FtsQ
CUST_2125_PI442896112 Cell division protein FtsW
CUST_839_PI442896112 Cell division protein MraZ
CUST_577_PI442896112 Cell division trigger factor
Functions related to adhesion
CUST_1669_PI442896112 Zinc metalloproteinase precursor
CUST_1668_PI442896112 Serine proteinase, V8 family
Functions related to proteolysis
3h
6h